Control Rod Shadowing and Anti-shadowing Effects

in a Large Gas-cooled Fast Reactor

G. Girardin*
Paul Scherrer Institute (PSI),
CH-5232 Villigen PSI, Switzerland
Tel: +41 56310264, Fax : +41 563102327, E-mail: gaetan.girardin@psi.ch

G. Rimpault
Commissariat à l'Energie Atomique (CEA), Cadarache,
13108 Saint-Paul-lez-Durance Cedex, France
Tel: +33 4 42257923, E-mail: gerald.rimpault@cea.fr

P. Coddington
Paul Scherrer Institute (PSI),
CH-5232 Villigen PSI, Switzerland
Phone: +41 563102738, Fax : +41 563102327, E-mail: paul.coddington@psi.ch

R. Chawla*
Paul Scherrer Institute (PSI),
CH-5232 Villigen PSI, Switzerland
Phone: +41 563102326, Fax : +41 563102327, E-mail: rakesh.chawla@psi.ch

Co-affiliation : Ecole Polytechnique Fédérale de Lausanne (EPFL), CH-1015 Lausanne, Switzerland

Abstract - *An investigation of control rod shadowing and anti-shadowing (interaction) effects has been carried out in the context of a design study of the control rod pattern for the large 2400 MWth Generation IV Gas-cooled Fast Reactor (GFR). For the calculations, the deterministic code system ERANOS-2.0 has been used, in association with a full core model including a European Fast Reactor (EFR)-type pattern for the control rods. More specifically, the core contains a total of 33 control (CSD) and safety (DSD) rods implemented in three banks: (1) a first bank of 6 CSD rods, placed at 64 cm from core centre in the inner fuel zone (Pu content 16.3 %$_{vol.}$), (2) a safety bank consisting of 9 DSD rods, at an average distance of 118 cm, and (3) a third bank with 18 CSD rods, placed at 171 cm, i.e. at the interface between the inner and outer (Pu content 19.2%$_{vol.}$) core regions. Each control rod has been modelled as a homogeneous material containing 90%-enriched B$_4$C, steel and helium.*

Considerable shadowing effects have been observed between the first bank and the safety bank, as also between individual rods within the first bank. Large anti-shadowing effects take place in an even greater number of the studied rod configurations. The largest interaction is between the two CSD banks, the anti-shadowing value δ being 46% in this case, implying that the total rod worth is increased by a factor of almost 2 when compared to the sum of the individual bank values. Additional investigations have been performed, in particular the computation of the first order eigenvalue and the eigenvalue separation. The main finding is that the interactions are lower when one of the control rod banks is located at a radial position corresponding to half the core radius.

I. INTRODUCTION

An investigation of control rod shadowing and anti-shadowing interaction-effects in a large 2400 MWth Gas-cooled Fast Reactor[1, 2] (GFR) has been performed and is presented in this paper. More precisely, the system selected for the current study is one of the advanced Generation IV reactors, currently being investigated by the Generation IV International Forum (GIF). It is in the context of a design study of the principal control rod pattern for this new reactor that the existence of significant control rod interactions has been observed and investigated.

Interactions between control rods (CRs) are observed when the reactivity worth of an absorber rod depends on the presence of another control rod in the surroundings. This phenomenon is also called shadowing or anti-shadowing effect, depending on whether the combined rod worth is decreased (positive shadowing) or increased (negative shadowing), respectively. The degree of shadowing or anti-shadowing is dependent on essentially the three-dimensional arrangement of the control rods and on the core geometry, particularly on the height-to-diameter ratio (H/D).

The analysis is based on the reference 2400 MWth GFR containing a total of 33 homogeneous European Fast Reactor (EFR) based control (CSD) and safety (DSD) rods implemented in three independent banks: (1) a first bank of 6 CSD rods, (2) a safety bank of 9 DSD rods, and (3) a third bank with 18 CSD rods. The implementation scheme is identical to that of EFR. The overall core dimensions are 1.55 m in height and 4.44 m in diameter.

To analyse the control rod interactions, the deterministic code system ERANOS-2.0 has been used in association with two different core models: (1) a RZ model including a control rod representation in homogenized rings and, (2) a HEX-Z model in which each sub-assembly is represented individually. Full core calculations – either with the 2D S_N-transport theory code BISTRO or the 3D nodal variational transport code VARIANT – were performed to compute the control rod worth (from eigenvalue differences) with respect to different configurations, e.g. (1) all rods withdrawn, (2) all rods inserted, or (3) insertion of individual rods.

First, Section II presents the 2400 MWth GFR models used in the study. Using these models, in conjunction with a reference computational scheme in ERANOS, the control rod worths were computed in order to analyse the different interactions occurring. Section III is devoted to the presentation and discussion of the calculated shadowing/anti-shadowing effects.

Additional investigations have been performed to predict and understand the origin of these control rod interactions and are discussed in Section IV, the first order

eigenvalue and the eigenvalue separation (SVP) being given particular consideration in this context. These have been found to be good indicators of the potential existence of CR interferences within the core. In order to compare the new GFR core with previously studied large fast reactors, reference is also made to corresponding neutronics analyses performed for commercial sodium-cooled fast-spectrum systems, viz. EFR and Super-Phénix. Conclusions for the paper are given in Section V.

II. GFR ERANOS MODELS

II.A. Main GFR Features

The large Generation IV GFR is a hard neutron spectrum, helium-cooled advanced reactor concept[2], with a thermal power of 2400 MW and an average power density of 100 MW/m^3. The use of high coolant temperatures, i.e. ~ 900°C, will permit an optimal thermal efficiency for electricity generation, as also greatly facilitate hydrogen production. On the fuel side, a new hexagonal sub-assembly design with new materials, such as SiC ceramic, are envisaged to accommodate the high temperatures. The core geometry is based on hexagonal plate-type sub-assemblies. The fuel is a ceramic-ceramic (CERCER) material consisting of (U, Pu)C placed in a SiC matrix. A sub-assembly is made of 3 different regions, each grouping parallel plates effectively enclosed in helium channels[3].

On the basis of the compositions and dimensions of the fuel plates within the fuel subassembly, the homogeneous volume fractions of the core are deduced as presented in Table I.

Table I
Composition (volume fractions) of the GFR.

Composition	Vol. %
(U,Pu)C	22.4
He, coolant	40.0
structural material	20.0
SiC matrix	6.4
He, gap in the plates	11.2

The core contains two zones of different Pu enrichments – 16.29% in the inner zone and 19.16% in the outer – the zones being almost equal in volume. The active fuel height is 1.55 m, corresponding to the axial coordinates z=1.00 to 2.55 m (for cold conditions). Radial and axial dilatations have been accounted for, axially assuming that the fissile content is linked to the matrix, and radially as governed by dilatation of the diagrid (assumed to be constructed in SiC).

The reflector materials is effectively a mixture of Zr_3Si_2 and helium, in different volume fractions, depending on the position: the axial reflector, above and below the fuel zones

(1 m thick), is made of 60% vol. Zr_3Si_2, the remaining volume being occupied by helium at 70 bar. The proportion is 80/20% for the radial reflectors. In addition, the central subassembly does not contain fissile material, but instead Zr_3Si_2 and helium in equal volume proportions, allowing one to reserve room for instrumentation or specific experiments. The control rods, implemented in three banks – 2 CSDs and 1 DSD, have been modelled in concentric rings by adjusting the thicknesses such as to preserve absorber volumes. In more detailed terms, the first CSD bank contains 6 rods, and the second one 18. There are 9 DSD rods in the intermediate safety bank, located at the core interface between the inner and outer core. The implementation scheme of the control rods is taken to be identical to that for EFR.

Specifically, a CR is modelled as a homogeneous mixture of steel, boron carbide and helium, the volume beneath (the rod follower mechanism) being considered as a homogeneous mixture of steel and helium.

II.B. RZ Model

To simplify the calculations and also to permit, for subsidiary studies, the use of perturbation theory in ERANOS[4, 5], calculations were first performed in association with a 2D RZ model. In the model, the three control rod banks were implemented in concentric rings, as mentioned above. Fig. 1 depicts the scheme adopted for the reference RZ GFR model.
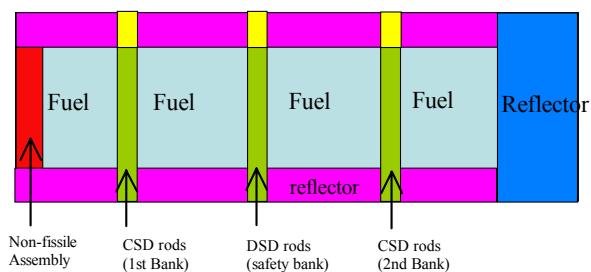

Fig. 1. RZ GFR core model.

For the calculations, self-shielded macroscopic cross-sections in 33 neutron groups were produced using the cell code ECCO, in conjunction with homogeneous cells and the adjusted ERALIB1[6] nuclear data library. The self-shielding is calculated in the fine 1968-group structure with the sub-group method. Then, in a second step, the core calculations were performed using the RZ transport-theory code BISTRO[7]. The numerical approximations used in BISTRO were P1/S16 for the order of the anisotropy of scattering and the angular discretisation of the flux, respectively.

The integral worth of a CR bank is obtained from the difference of the eigenvalues for the bank fully withdrawn and the same bank fully inserted.

II.C. HEX-Z Model

A 3D HEX-Z full core model was used in conjunction with the 3D nodal variational code VARIANT[8], in order to model each sub-assembly, and hence each control rod, individually (Fig. 2). This also allows one to compute the worth of each rod separately, which is clearly not possible using the simplified RZ model. Even more important, the control rod geometry can be preserved accurately this time.
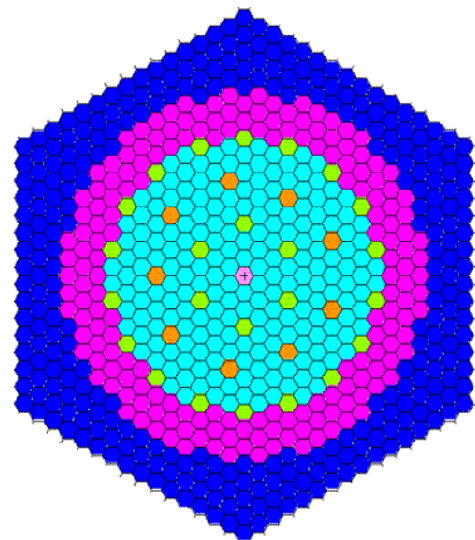

Fig. 2. 3D HEX-Z GFR model in ERANOS. The three (CSD in green, DSD in orange) banks are shown explicitly, in addition to the central non-fissile sub-assembly. At the periphery, the reflector is shown in dark blue. The two different fuel zones are represented in light blue and pink.

The macroscopic cross-sections were computed the same way as for the RZ model albeit, in the second step, the flux was computed with VARIANT[8]. The numerical approximations in VARIANT for the flux calculations were those of set "601", viz.:

- transport calculation with simplified spherical harmonics,
- order of polynomial expansion for nodal source of 1,
- order of polynomial expansion for even flux of 6,
- order of polynomial expansion for partial current (leakage) of 0.

Both with the RZ and HEX-Z models, the calculations were performed for operating, i.e. "hot", conditions[3]. Table II provides the corresponding temperatures used in the calculations.

Table II
Material temperatures.

Material	Temperature, °C
Inlet Helium	480
Outlet Helium	850
Fuel	990
Structures	665

In general terms, eigenvalues and control rod worths, as also the sensitivity of the latter to the modelling and the main computational options, were assessed. In order to assess the sensitivity, four CR configurations were defined and the following computational options were tested:

- nuclear data library: the adjusted ERALIB1 and the JECCOLIB2 (based on JEF-2.2) data libraries,
- operating conditions: "hot" and "cold" conditions in association with the HEX-Z model,
- transport or diffusion theory, in association with the RZ BISTRO model,
- the HEX-Z versus the RZ model, both with transport theory.

Based upon the results, it was found that:

- the sensitivity of the CR worth to the choice of the nuclear data library and to the operating conditions is rather limited: ~0.3% and ~0.1%, respectively. This confirms that one may perform the CR interaction analysis without significant dependence on the operating conditions and/or the data set
- the eigenvalues and the control rod worths are very sensitive to the core modelling, i.e. RZ versus HEX-Z (see Table III), and to the computational options, i.e. diffusion versus transport theory, the bank worth sensitivity for these two typically being ~20% and 4%, respectively.

However, it is important to stress that, even if the CR worths are highly sensitive to the modelling, significant control rod interactions are observed in all cases, i.e. with all computational options (see Table III).

Table III
Sensitivity of the control rod worth to the use of the RZ and HEX-Z models, both considered for operating "hot" conditions.

Configuration	Worth, pcm	
	HEX-Z	RZ
All CSD Rods inserted	15462	18518
1st bank inserted	2293	2648
2nd bank inserted	6164	6199

III. CONTROL ROD INTERACTIONS

The control rod interactions have been analysed using the HEX-Z model, in conjunction with nodal flux calculations to compute the control rod worths with respect to different control rod configurations. As mentioned earlier, the two main parameters used for characterising the interactions are: (1) the rod interaction effect δ, and (2) the amplification factor A. The definitions are provided below.

III.A. Definitions

In effect, shadowing and anti-shadowing effects, or interactions between control rods, are associated with the modification, as a consequence of the presence of other CRs, of the nominal worth of a given control rod. The control rod interaction is defined as the relative difference between the value of the total worth of a group of control rods and the sum of the individual worths. Thus, if there are N control rods (or banks), each with a reactivity worth $\Delta\rho_i$, then the rod (or bank) interaction effect[9] δ is given by:

$$\delta \equiv \frac{\Delta\rho_{1,2,...N} - \sum_{i=1}^{N} \Delta\rho_i}{\Delta\rho_{1,2,...N}} \qquad (1)$$

If $\delta \neq 0$, then there is some interaction and in this case there are two possibilities, i.e. $\delta < 0$ and $\delta > 0$. The case $\delta < 0$ corresponds to a shadowing effect, where a control rod in a certain location can reduce the reactivity worth of another rod. The situation with $\delta > 0$ corresponds to anti-shadowing, the combined worth being greater than the sum of the individual worths.

In addition to this definition, another parameter called the amplification factor (A) of control rod J, is defined by Eq. (2), viz.

$$A_J = \frac{\Delta\rho_{1,2,...J} - \Delta\rho_{1,2,...J-1}}{\Delta\rho_J} \qquad (2)$$

where $\Delta\rho_{1,2,\dots J}$ is the total worth of all rods (1 to J), $\Delta\rho_{1,2,\dots J-1}$ the total rod worth of the rods 1 to J-1 and $\Delta\rho_J$ the worth of the single rod J.

If A_J is >1, the control rod worth is amplified, and this corresponds to an anti-shadowing effect, while if A_J is <1, the rod worth is reduced and one has a shadowing effect.

III.B. Results for the GFR Core

Both the above parameters permit the quantification of the degree of interaction in the GFR core, between the different CR banks, as well as between the individual rods within a given bank. Consequently, calculations have been carried out for various combinations of inserted CR banks (see Table IV), the corresponding inserted-bank reactivity worths allowing one to quantify the diverse interactions in terms of δ and A_J values.

Table IV
Control rod bank configurations and corresponding worths

Configurations	1st CSD	DSD	2nd CSD	R. worth, pcm
Both CSD inserted	in	out	in	15598
1st CSD inserted	in	out	out	2372
2nd CSD inserted	out	out	in	6052
DSD inserted	out	in	out	4788
Both CSD and DSD	in	in	in	19171
1st CSD and DSD	in	in	out	5553
2nd CSD and DSD	out	in	in	11818

The CR-bank interactions are presented in Table V and show quite different effects for the different cases. Thus, large anti-shadowing effects take place between the two CSD banks (δ = 46%), as well as between the DSD and the two CSD banks taken separately (δ = 31%). For the interaction between the DSD and the second CSD alone, the effects are more limited (δ = 8%).

Table V
Control rod bank interactions (δ).

Bank Interaction	δ, %
Between 1st CSD and 2nd CSD	46
Between DSD and both CSD	31
Between DSD and 1st CSD	-29
Between DSD and 2nd CSD	8

For the largest interaction case, i.e. that between the two CSD banks (δ = 46%), the total worth (15598 pcm) is increased by a factor of almost 2, as compared to the sum (8424 pcm) of the individual bank values (2372 pcm for the first CSD bank and 6052 pcm for the second). In the case of the interaction between the DSD and the first CSD bank on its own, one has a large shadowing effect (δ = -29%

Table VI gives the amplification factors for the individual banks for selected cases.

Table VI
Amplification factors (A_j) for selected cases.

Bank	Case	A_J
1st CSD	In conjunction with 2nd CSD	4.0
2nd CSD	In conjunction with 1st CSD	2.2
DSD	In conjunction with 1st CSD	0.7

The values in Table VI confirm the fact that each CSD bank amplifies the worth of the other CSD bank (A_J = 4.0 and 2.2). On the other hand, the amplification factor of the safety bank, viewed in conjunction with the 1st CSD is 0.7, implying a shadowing effect and consistent with the corresponding negative δ value in Table V.

Table VII shows the interactions at the level of individual rods within the different control rod banks. Shadowing effects are observed for the rods within the first CSD bank (δ = -34%), while anti-shadowing effects are seen for the other two cases (δ = 11% for the effects within the 2nd CSD bank, and δ = 20% for the DSD rods). For the first CSD bank, the shadowing leads to a reduction of the individual control rod worth from 530 pcm (the value derived from the insertion of a single CSD rod) to 395 pcm, the average worth per rod considering insertion of the entire bank ($\Delta\rho$ = 2370 pcm for all 6 CSDs inserted).

Table VII
Interactions (δ) for individual rods in the different banks.

Configuration	δ, %
First CSD bank	-34
Second CSD bank	11
DSD rods	20

From a study of Tables V-VII, it is seen that the various interactions, at both bank and individual rod levels, are dependent, in a complex manner, on several different factors (location, number of rods, type of other bank/rod, etc.). Certain supplementary studies showed that there are, in principle, possible ways to reduce the interaction effects drastically, but these are not practical in most cases. Thus, for example, if one were to group the control rods belonging to the two CSD banks, such that half the 1st-CSD-bank rods were grouped with half the 2nd-CSD-bank rods, one would have two new "banks", for which the anti-

shadowing would be as low as 5%. However, such a cross-linking of rods belonging to different "rings" would not be able to meet power flattening requirements in a satisfactory manner.

III.C. Neutron flux traverses

The introduction of the different CR banks significantly affects the radial neutron flux profile, which is essentially the basic reason for the amplification of bank worths indicated in Table VI. To investigate the origin of these large interactions more closely, radial traverses of the neutron flux and fission power were computed for the four main configurations: (1) all rods withdrawn, (2) all CSD rods inserted, (3) only the first CSD bank inserted, and (4) only the second CSD bank inserted.

Figs. 3 and 4 show the radial flux and power distributions, respectively, for the different cases and illustrate that the movement of an individual CSD bank leads to a large displacement in the neutron flux. This effect is clearest for the second CSD bank, where the flux is shifted from the core periphery towards the centre. In Fig. 4, it is seen that the form factor becomes very high – about 3 – when the second CSD bank is introduced, which is not acceptable for obvious safety reasons.
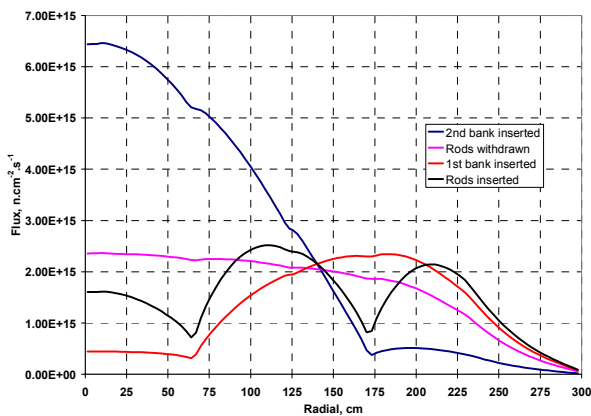

Fig. 3. Radial traverses of the neutron flux at mid-core with respect to four control rod bank positions: (1) all rods withdrawn, (2) all CSD rods inserted, (3) only the first CSD bank inserted, and (4) only the second CSD bank inserted.
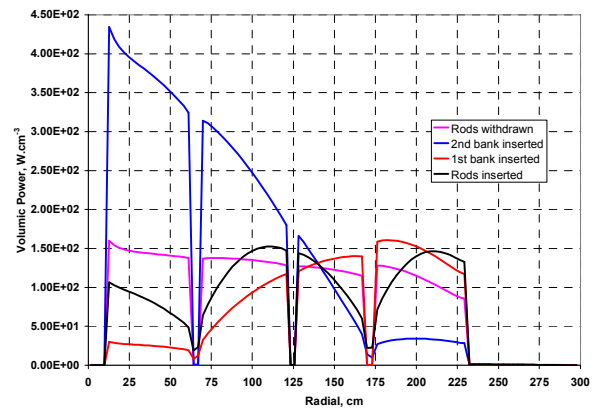

Fig. 4. Radial traverses of the fission power at mid-core with respect to the four control rod bank positions considered in Fig. 3.

It is important to stress that these observations (shift of the flux) are consistent with measured values from Super-Phénix, confirming the existence of the phenomenon. Similar observations have also been made for various test reactors[10, 11].

IV. EIGENVALUE SEPARATION (SVP)

Additional investigations have been performed using the 2D model to determine the first order eigenvalue and the eigenvalue separation[12] SVP, defined by the following equation:

$$SVP \equiv \frac{1}{1 - \dfrac{k_{Order1}}{k_{Fundamental}}} \qquad (3)$$

where k_{order1} is the eigenvalue corresponding to the first harmonic and $k_{fundamental}$ is the fundamental eigenvalue. The calculations were performed with BISTRO[7] using transport theory.

A large SVP value means that the magnitude of the first order eigenvalue is comparable to the fundamental eigenvalue and consequently leads to neutronic instabilities and power oscillations[12, 13]. The importance of harmonics is principally correlated to the overall core dimensions or to the height-to-diameter ratio (H/D), as also to the average mean free path over the whole core. With a low H/D ratio, the harmonics can be propagated more easily within the core.

The SVP values have been computed for two control rod bank configurations: (1) all rods withdrawn and (2) only the second CSD bank inserted, and the results are presented in Table VIII.

Table VIII
Eigenvalue separation (SVP) with respect to two control rod bank configurations: (1) all rods withdrawn, and (2) only the second CSD bank inserted.

Configuration	SVP	k_{eff}, fund.	k_{eff}, 1st order
Rods withdrawn	8.2	1.1030	0.9688
2nd CSD bank inserted	7.0	1.0336	0.8865

It is seen that the SVP value of 8.2 (all rods withdrawn) is large and is reduced when the absorbers are inserted, i.e. a SVP value of 7.0 for the 2nd CSD bank inserted configuration. This reduction is to be expected since the insertion of an absorber would inhibit the propagation of harmonics within the core, corroborating the statement made above.

In previous studies, performed for Super-Phénix, the SVP value calculated was 10.5 and large CR interactions were measured. In the EFR, the SVP value was even higher at 13.6. As a consequence, and taking into account the current GFR analysis, one has a clear confirmation that a high SVP value is a good indicator of the potential existence of large control rod interactions. The advantage of such a criterion is that it provides an easy method to assess the likelihood of interactions and core instabilities.

It is important to stress that alternative GFR core designs are under investigation, with a larger height and a smaller diameter, e.g. with a H/D of 0.6 instead of the present 0.35, in order to increase primarily the breeding gain and to reduce the neutron leakage, for a better neutron economy. The increase of the H/D ratio will, in turn, have a positive effect in reducing the strong neutronic instabilities, due to large CR interactions observed in the reference GFR core.

Additionally, the SVP value impacts the number of CRs. For instance, to limit the power oscillations due to the movement of a CR, it is necessary, to implement a high number of absorbers and to limit the speed of movement of these rods. Finally, the SVP also impacts the core instrumentation, with the need to measure the flux at a large number of locations in order to detect rapid changes in the power distribution.

Complementary to the SVP values, the radial power distributions of the fundamental and first order eigenvalue for the two configurations are depicted in Figs. 5 and 6.

A differential behaviour is observed for the first order eigenvalue, with a negative contribution in the inner core region, which then crosses the axis and becomes positive. An interesting finding is that the sign changes at the current location of the DSD rods, which means that the amplitude of the harmonics is minimal at that location. This suggests that the DSD rods, placed at 1.18 m (mid-core, r/R = 0.53) from the core centre, minimise the interactions with other control rods. The amplification factor of the DSD rods, i.e.

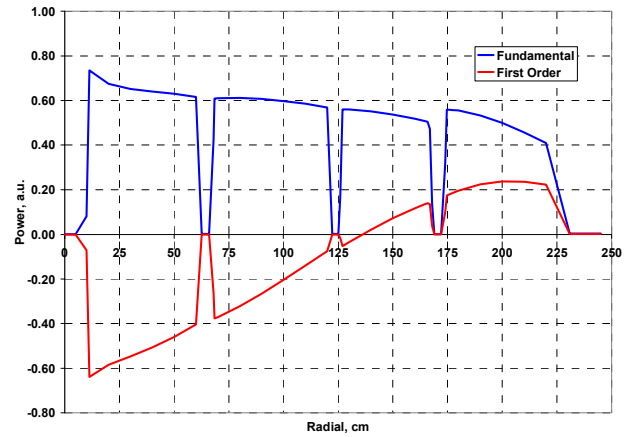0.7, confirms this finding (see Table VI), because this is the smallest of the amplification factors computed.

Fig. 5. Radial power distribution at mid-core of the fundamental and first order eigenvalues for the "all rods withdrawn" configuration.
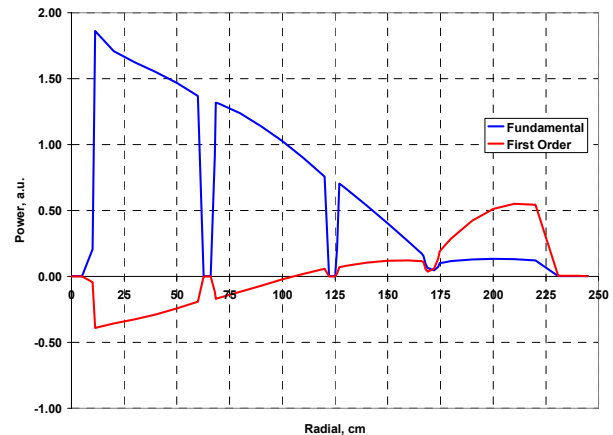

Fig. 6. Radial power distribution at mid-core of the fundamental and first order eigenvalues for the "only second CSD bank inserted" configuration.

V. CONCLUSIONS

An investigation of control rod shadowing and anti-shadowing effects in the large 2400 MWth Generation IV Gas-cooled Fast Reactor has been presented in this paper. The control rod interactions, both between the banks, and the individual rods, have been characterized by means of the interaction effect δ and amplification factors A_j. Specifically, while significant shadowing effects are observed in certain cases, large anti-shadowing effects occur in even more of the control rod configurations studied. The largest interaction is found between the two CSD banks, the anti-shadowing value being 46% in this case, implying that the total rod worth is increased by a

factor of almost 2 compared to the sum of the individual bank values.

Additionally, the potential existence of neutronic instabilities due to control rod movements has been analysed. For this purpose, the fundamental/first-order eigenvalues, and the eigenvalue separation (SVP), were computed. The SVP value gives an indication of the importance of harmonics, relative to the fundamental mode. It was found that, consistent with other large fast systems (for example, Super-Phénix for which SVP = ~ 10), the GFR has a high SVP value, viz. ~ 8. This is clearly a strong indication of the potential existence of large CR interactions. Another finding is that the radial power distribution corresponding to the first order eigenvalue exhibits a local minimum at the mid-core radius, confirming the optimal current location of the safety bank.

More generally, the SVP value is dependent on the average mean free path of the neutrons and the core dimensions, particularly the height-to-diameter ratio (H/D), a large ratio being favourable for lowering the CR interactions. Accordingly, alternative GFR core designs, with a larger height and a smaller diameter, are now being considered, with a view to reducing the currently reported large CR interactions.

REFERENCES

1. J. Rouault and T.Y.C. Wei, "The Gen-IV gas-cooled fast reactor, status of studies", Proc. Workshop on Advanced Reactors with Innovative Fuels, ARWIF, Oak Ridge, USA (2005).

2. R. Jacqmin, "Gas-cooled Reactor Core Physics R&D Activities in France", Gen-IV Reactor Physics Workshop, PHYSOR 2004, Chicago, April 30 (2004).

3. J.C. Bosq et al., "Fine 3D neutronic characterization of a gas-cooled fast reactor based on plate-type sub-assemblies", ANS Topical Meeting on Reactor Physics, PHYSOR-2006, Vancouver (2006).

4. J. Y. Doriath et al., "ERANOS 1: The Advanced European System of Codes for Reactor Physics Calculations", Joint Conference on Mathematical Methods and Supercomputing in Nuclear Applications, Karlsruhe, Germany (1993).

5. G. Rimpault et al., "The ERANOS Data and Code System for Fast Reactor Neutronic Analyses", Int. Conf. On the New Frontier of Nuclear Technology: Reactor Physics, Safety and High-Performance Computing, PHYSOR, Seoul, Korea (2002).

6. E. Fort et al., "Improved performances of the fast reactor calculational system ERANOS-ERALIB1 due to improved a priori nuclear data and consideration of specific additional data", Annals of Nuclear Energy 30, p. 1879-1898 (2003).

7. C. J. Gho and G. Palmiotti, "BISTRO: Bidimensionnel SN transport optimisé. Un programme bidimensionnel de transport SN aux différences finies, Note No 1: Définition des algorithmes pour la géométrie X-Y", Note Technique, CEA, SPRC/LEPh 84-270 (1984).

8. G. Palmiotti et al., "VARIANT: Variational Anisotropic Nodal Transport for Multidimensional Cartesian and Hexagonal Geometry Calculation", Technical Report, ANL-95/40, Argonne National Laboratory (1995).

9. T. Taryo et al., "Investigation on Control Rod Interaction in a Conceptual MTR-Type Reactor", IAEA-CN-100/90P, Research Reactor Utilization, Safety, Decommissioning, Fuel and Waste Management, Int. Conference, Santiago, Chile (November 2003).

10. M. Itagaki et al., "Control-Rod Interference Effects Observed During Reactor Physics Experiments With Nuclear Ship MUTSU", J. Nucl. Sci. Technol. (Jpn.). Vol. 30, no. 5, pp. 465-476 (May 1993).

11. M. A. Ghafoor, P. J. Grant, "An experimental study of the interactions between control rods in a subcritical assembly", Brit. J. Appl. Phys., Vol. 15 (1964).

12. T. Kitada, T. Takeda, "Evaluation of Eigenvalue Separation by the Monte Carlo Method", Journal of Nuclear Science and Technology, Vol. 39, No. 2, p. 129-137 (February 2002).

13. G. Aliberti, "Caractérisation neutronique des systèmes hybrides en régimes stationnaires et transitoires", Université Louis Pasteur de Strasburg, Thèse (2001).

14. D. Honde et al., "ERANOS: Manuel des Méthodes, Les calculs de perturbations et les analyses de sensibilité", Note Technique CEA, SPRC/LEPh 96-205 (1996).